2014 23rd International Lightning Detection Conference
18 - 19 March • Tucson, Arizona, USA
5th International Lightning Meteorology Conference
20 - 21 March • Tucson, Arizona, USA

Predicting Heavy Precipitation and Lightning for a Mesoscale Convective System Case Over Southern Brazil

Zepka G. S., Azambuja R. R., Vargas Jr. V. R., Saraiva A. C. V., Pinto Jr. O.
ELAT/CCST, Atmospheric Electricity Group
INPE, National Institute for Space Research
São José dos Campos, SP, Brazil
E-mail: giselezepka@gmail.com

Abstract— **On December 10th through 11th 2012, a strong convection activity over southern Brazil grew into a huge Mesoscale Convective System (MCS) accompanied by heavy precipitation, hailstorm, damaging winds and dangerous lightning. The Civil Defense Authority reported that over 700,000 people experienced power outages due to either strong winds or lightning strikes or even suffered from flash floods caused by high rain volumes. The Brazilian Lightning Location System (BrasilDAT) detected more than 90,000 cloud-to-ground (CG) lightning strikes during the MCS activity, and approximately 4,000 CG strokes presented large peak currents over 75 kA. The main objectives of this work were to achieve the most suitable configuration of the Weather Research and Forecasting (WRF) model, and to apply the Potential Lightning Region (PLR) tool, in order to forecast reliably this type of severe weather event with enough time in advance to adopt strategies that might minimize injuries and hazardous situations in the future. Firstly, the CG and IC lightning stroke rates, the peak currents distribution, and the IC/CG ratio were evaluated. Observed precipitation from a homogeneous network of surface meteorological stations was used as proxy data. Lightning and precipitation were compared during the MCS development in order to seek for correlations. As well known, current operational models cannot predict convective subgrid scale processes explicitly, due to their microscopic and discontinuous nature, and must do so via parameterization. In this case, a cumulus scheme should try to transport heat vertically, redistribute moisture, and reduce thermodynamic instability. Four cumulus parameterization schemes (CPS) in the WRFv3.3.1 model were investigated to proper simulate this MCS over southern Brazil. WRF grid points near meteorological stations with high accumulated precipitation values were chosen in order to assess the behavior of the simulated data against the observations. The Potential Lightning Region (PLR) is a tool that indicates the spatial distribution of lightning occurrence probabilities in a given area. PLR was developed from a combination of WRF output variables, and operationally tested over southeastern Brazil. The WRF convective parameterization selected from the previous analysis was used to generate new PLR maps over southern Brazil for the MCS. This case study served as a laboratory to expand PLR capabilities in the prediction of severe weather events.**

Keywords— lightning; precipitation; Mesoscale Convective System; WRF model; PLR; cumulus parameterizations

I. INTRODUCTION

Mesoscale Convective Systems (MCSs) consist of a particularly well-organized cluster of clouds in different stages of life cycle that produce a contiguous area of convective and stratiform precipitation which can extend for several hours with a horizontal extension of at least 100 km [Houze, 1993]. These large thunderstorms are substantial producers of rainfall and lightning in the tropics and mid-latitudes during the warm season. In South America, MCSs are frequently found between the 20° S and 40° S latitudes, including Paraguay, Uruguay, northeastern Argentina, and southern Brazil [Velasco and Fritsch, 1987; Machado et al., 1998; Siqueira et al., 2005; Silva and Berbery, 2006; Teixeira and Satyamurty, 2007]. This is mainly due to the strong advection of warm, moist air provided by the South American Low-Level Jet (SALLJ) on the east of the Andes during the spring and summer seasons [Velasco and Fritsch, 1987; Marengo et al., 2004]. Several studies have reported the cloud-to-ground (CG) lightning activity in MCSs around the world [e.g. Goodman and MacGorman, 1986; Orville et al., 1988; Rutledge and MacGorman, 1988; Keighton et al., 1991; Holle et al., 1994; MacGorman and Morgenstern, 1998; Parker et al., 2001; Carey et al., 2005]. The southern and southeastern Brazil is known for having high incidence of cloud-to-ground (CG) lightning flashes that are usually associated with the passage of MCSs [Nesbitt et al., 2000; Abdoulaev et al., 2001; Pinto Jr. et al., 2004; Zipser et al., 2006; Mattos and Machado, 2011].

In spite of their substantial contribution to the production of significant weather, MCSs are not forecast very well [Corfidi

Sponsored by FAPESP (Fundação de Amparo à Pesquisa do Estado de São Paulo) under grant numbers 08/56711-4 and 2011/17806-2.

et al., 1996]. Size, movement, and lifetime of these convective clusters are often critical to a good forecast. In South America, the mechanisms behind the formation of MCSs are poorly understood mainly due to a lack of observational data coverage in areas where such systems take place, except in periods in which field experiments occur. The option is the use of regional models; but experiments with regional models for predicting MCSs during SALLJEX (South American Low-Level Jet Experiment) [Vera et al., 2006] show that still there is some deficiency as regards to the position and intensity of these systems predicted by models. This is probably related to the lack of observations assimilated by analyzes, especially along the Andes, or the low resolution of the models that do not simulate well the aspects of mesoscale and local circulations.

The purpose of this paper is to evaluate and discuss the performance of the Weather Research and Forecasting (WRF) model in predicting the heavy precipitation and the lightning activity produced by a huge MCS that occurred over southern Brazil in the middle of December 2012. Firstly, the synoptic conditions responsible by the MCS occurrence were presented and discussed. Cloud-to-ground (CG) and intracloud (IC) lightning distributions through the life cycle of this MCS were analyzed and compared with observed rainfall data to seek for correlations. The polarity and peak currents of CG strokes were also investigated. Simulations were performed using different cumulus parameterizations on WRF model, in order to check for the best match with the observed precipitation. Finally, the Potential Lightning Region (PLR) tool [Zepka et al., 2014] was used to forecast the areas with probability of lightning occurrence associated with the MCS. For the first time, PLR was tested for a region different from southeastern Brazil, where it was conceived and is used operationally.

II. METEOROLOGICAL SCENARIO

From December 10th until 11th 2012, severe convective storms took shape over Argentina, Uruguay and southern Brazil (Fig. 1) leaving injury and destruction in their wake. As a result of a combination of different weather conditions, a strong convection activity growing into a huge mesoscale convective system associated with cyclogenesis. The synoptic situation was briefly analyzed using surface and upper air charts from CPTEC (Center for Weather Forecasting and Climate Research/Brazil), IR (infrared) satellite image and radar data. In Fig. 2, the 250mb chart (for 12/11/2012 at 00Z) showed a predominant anticyclonic pattern in most of Brazil that was induced by the presence of the Bolivian High (BH) over the northern Argentina (18°S/70°W), and the Subtropical Jet Stream (STJ) over the Río De La Plata Basin. As a consequence, intense difluence was induced which, along with the passage of shortwave troughs in southern Brazil, enhanced convection and increased the instability of the lower-troposphere over Rio Grande do Sul (RS) state. In the 850mb chart (Fig. 3), a flow with speed exceeding 20 knots is noted between southern Bolivia and northern-central Argentina, indicating the performance of SALLJ in making the atmosphere even more unstable with the transport of heat and moisture from northward to southern Brazil. At surface (Fig. 4), it is possible to observe a strong temperature gradient between north-northeastern Argentina and southern Uruguay, where a cold front moved rapidly northeastward driven by a minimum low-pressure of 996 hPa at 40°S/53°W. The GOES13-IR satellite image (Fig. 5) at 0130UT for 12/11/2012 shows strong convection associated to the MCS over southern Brazil. Intense precipitation cells were observed by Canguçu Radar (located in the city of Canguçu/RS – 31°S/52°W) for the same time period (Fig. 6). The reflectivity data is an integrated CAPPI (Constant Altitude Plan Position Indicator) image.

Fig. 1. Geographical map with the location of Rio Grande do Sul state (southern Brazil). Region of interest from where the lightning and the observational data were analyzed. (pt.wikipedia.org/wiki/Ficheiro:RioGrandedoSul_MesoMicroMunicip.svg)

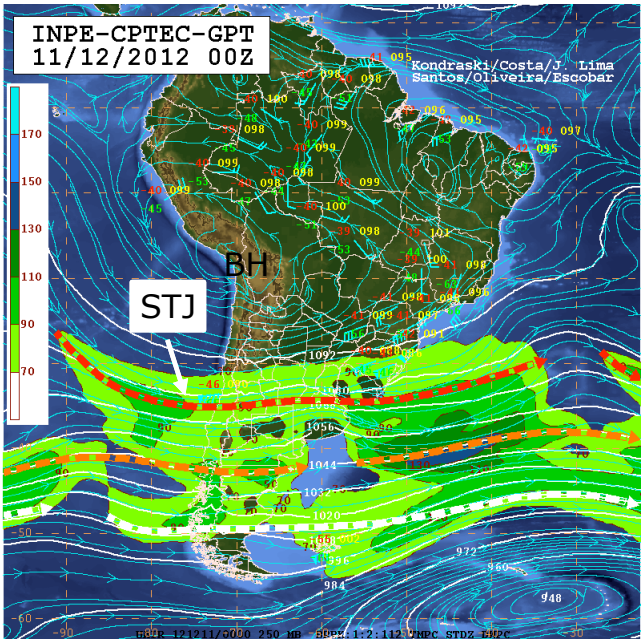

Fig. 2. 250mb chart. The locations of the Bolivian High (BH) and the Subtropical Jet Stream (STJ) are indicated on the map. Rio Grande do Sul (RS) is the southmost state of Brazil.

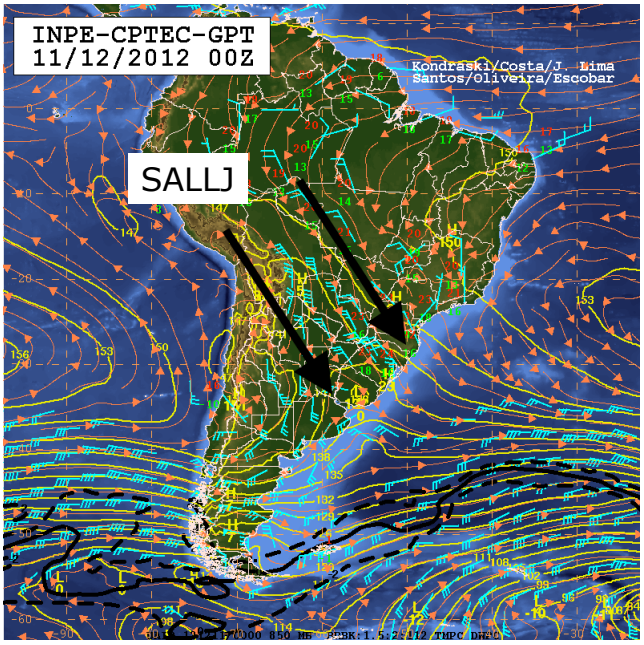

Fig. 3. 850mb chart. The South American Low-Level Jet (SALLJ) is indicated on the map.

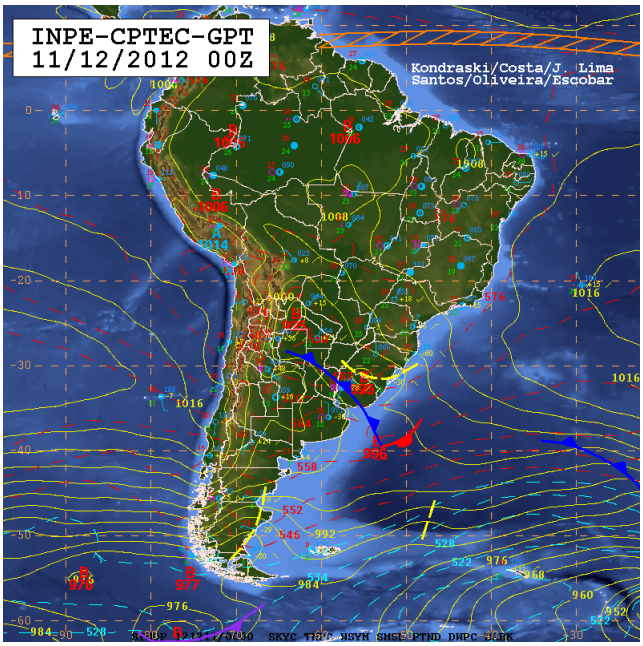

Fig. 4. Surface pressure chart.

Heavy precipitation, hailstorm, damaging winds, and strong lightning activity were reported from the regions where the MCS passed through. The Civil Defense Authority of Rio Grande do Sul state reported that over 700,000 people experienced power outages due to either strong winds or lightning strikes or even suffered from flash floods caused by high rain volumes. Figs. 7 and 8 illustrate two cases of damage caused by the MCS that were recorded by a local newspaper.

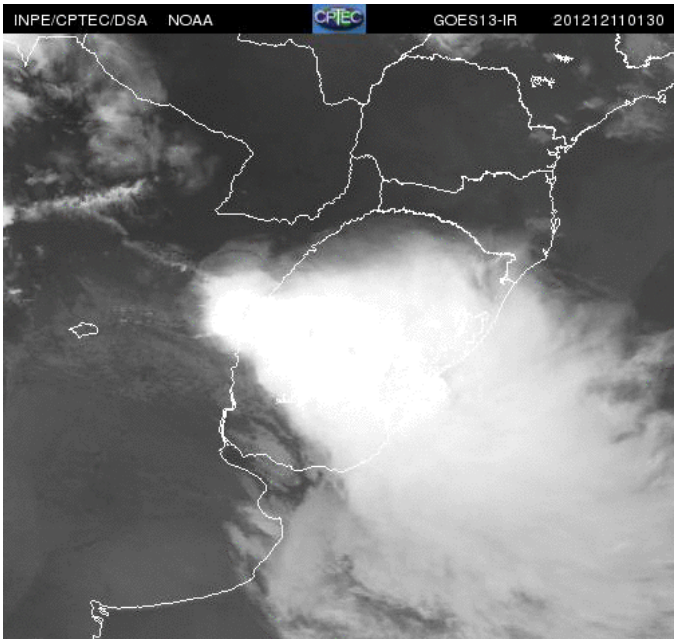

Fig. 5. GOES13-IR satellite image at 0130UT on December 11th, 2012 showing the MCS passing through Uruguay and Rio Grande do Sul state.

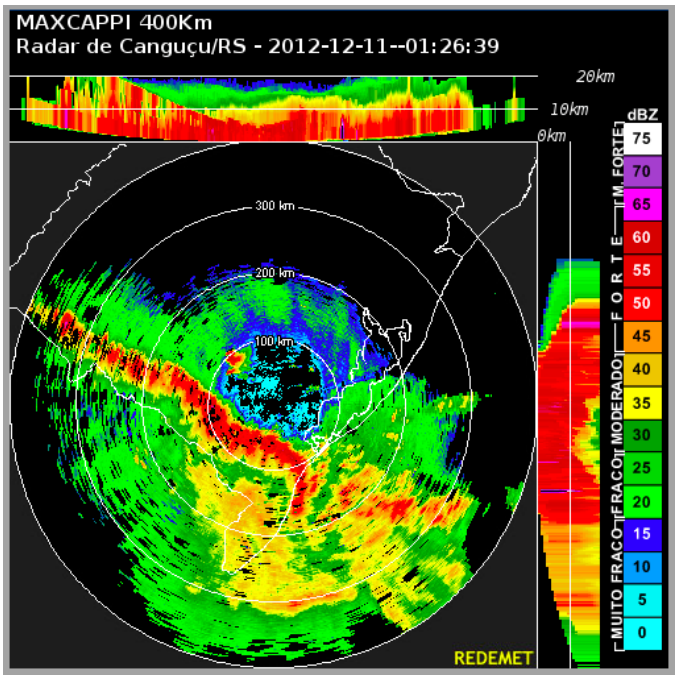

Fig. 6. MaxCAPPI radar image at 0126UT on December 11th, 2012 indicating the high reflectivity band associated with heavy precipitation of the MCS. The radar data is available by Rede de Meteorologia do Comando da Aeronáutica (REDEMET, http://www.redemet.aer.mil.br).

III. TOTAL LIGHTNING FROM BRASILDAT

The BrasilDAT Network is a lightning detection network based on the *EarthNetworks* Total Lightning System (ENTLS), which is an integrated total lightning detection system that combines wide-band sensors and relative dense network deployment to detect both IC and CG discharges simultaneously. The BrasilDAT deployment started in

December 2010 and now is composed by 56 sensors covering the southeastern, southern, center and part of northeastern Brazil. Some theoretical calculations show that BrasilDAT has presently 85% to 90% CG detection efficiency, about 50% to 60% IC detection efficiency, and about 500 m CG location accuracy in southeastern Brazil [Naccarato et al., 2012]. No study has yet been published regarding these estimates for the region of interest in this paper. In the following analysis, the values used for the CG and IC detection efficiency (DE) are based on some case studies still under development.

Fig. 7. Photo recorded by a local newspaper showing that the winds were strong enough to uproot the tree (http://zerohora.clicrbs.com.br/rs/fotos/veja-fotos-do-mau-tempo-no-rs-durante-a-madrugada-34544.html).

Fig. 8. Photo recorded by a local newspaper showing a house that caught fire after a short-circuit in the power network caused by lightning strike (http://zerohora.clicrbs.com.br/rs/fotos/veja-fotos-do-mau-tempo-no-rs-durante-a-madrugada-34544.html).

CG and IC lightning data provided by BrasilDAT for the Rio Grande do Sul area (see Fig. 1), from December 10th until 11th 2012, were used in this study. Six sensors cover the RS state and participate in the solutions. Fig. 9 shows the temporal distribution of CG and IC lightning strokes for the whole period of the MCS activity over southern Brazil. The CG and IC discharges registered by BrasilDAT are represented by the black and orange histograms, respectively. It is possible to observe that the maximum activity of CG (11,602 strokes) occurred in the early morning of the day 11, exceeding the peak IC activity (10,430 strokes) verified hours later. As the detection efficiency (DE) of BrasilDAT is different for CG and IC, both rates must be corrected. It was assumed a DE~90% for CG strokes and a DE~40% for IC. After correction, the new curves were added in Fig. 9: black, indicating the behavior of CG strokes, and orange, the activity of IC. The corrected temporal evolution starts with peak IC activity changing to predominant CG activity and concluding with a substantial number of IC strokes before the total dissipation of the MCS. The most vigorous period of the MCS corresponded to the first maximum of CG and IC strokes.

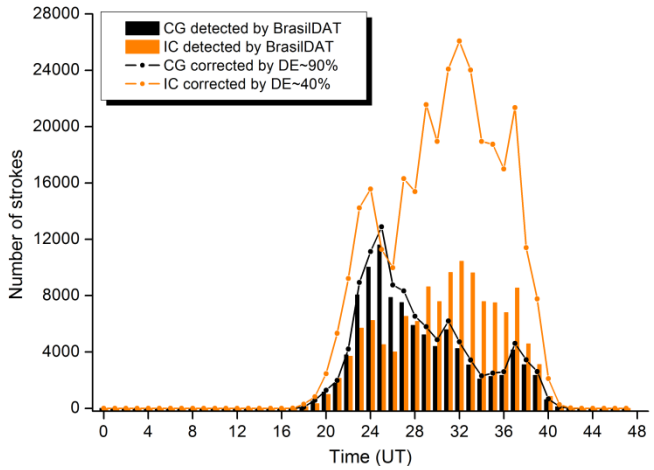

Fig. 9. Temporal evolution of CG and IC strokes during the MCS activity over southern Brazil. The lightning data were corrected according to the estimated DE of BrasilDAT for CG and IC in the region of interest.

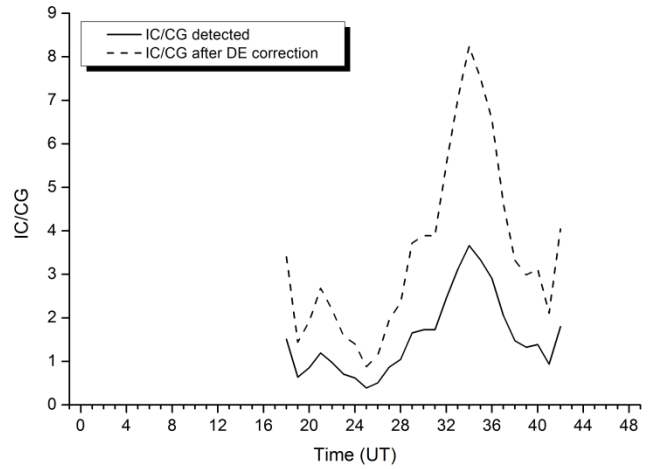

Fig. 10. Temporal evolution of IC/CG ratio before and after DE correction.

Fig. 10 shows the behavior of the IC/CG ratio during the passage of the MCS. Considering the number of CG and IC strokes corrected by DE, the average IC/CG for the entire

period was 3.5, and the maximum, 8.2. Pinto Jr. et al. [2007] compared maximum CG lightning flash densities, provided by a Lightning Location System different from BrasilDAT, with total lightning observations by satellite to infer the IC/CG ratio in southeastern Brazil. The value encountered was 4.9. Since BrasilDAT was recently installed in Brazil, there are not enough data to calculate the IC/CG ratio based on the CG and IC discharges detected so far.

Fig. 11 shows the peak currents distribution of 97,696 negative and positive CG strokes observed during the overall period analyzed. More than 80% of strokes were negative. Lyons et al. [1998] arbitrarily defined CG lightning flashes with large peak current (LPCCG) as those with peak currents >75 kA. For this MCS, 4% of the CG strokes were LPCCG, and almost 30%, positive. However, it is important to note that lightning data used in this work are strokes, not flashes, and the BrasilDAT technology is different from the LLS used by Lyons et al. [1998].

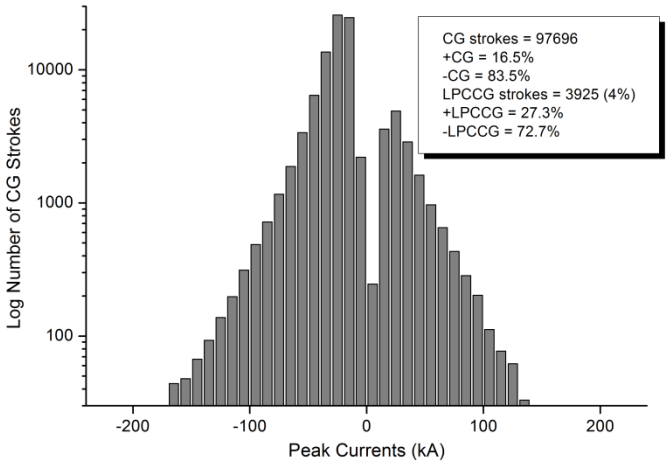

Fig. 11. Peak currents distribution of negative and positive CG strokes. The caption presents some statistics regarding the LPCCG observed.

A. Lightning Vs. Precipitation Data

Several cities of RS state reported the occurrence of heavy rainfall associated with the MCS. Seeking a temporal relationship, lightning activity was compared with accumulated amount of hourly-observed precipitation collected of 50 surface weather stations from National Institute of Meteorology (INMET). The stations are homogeneously distributed throughout the study area, as shown in Fig. 12.

During the 24-hours of the MCS activity (from 18UT of December 10th to 18 UT of December 11th) over the study area, the average hourly precipitation recorded was 45.3 mm, and the accumulated for the entire period, 1132.4 mm. Analyzing Fig. 13, it is possible to observe that the highest number of CG strokes (about 13,000) preceded the peak precipitation of approximately 160 mm. In just one hour, this cumulative rainfall across the region exceeded, for example, the monthly average precipitation expected for December (100 mm) in the city of Porto Alegre (capital of the RS state, represented by the station A801). After that, as the CG activity decreases over time, the precipitation increases accompanied by IC strokes. The second maximum of precipitation (145 mm) matched with the peak IC strokes (more than 26,000). Even at the end (at 37UT) of the MCS propagation, when precipitation had fallen, there were more two peaks in the activity of CG and IC. (2300 and 18,950 strokes, respectively).

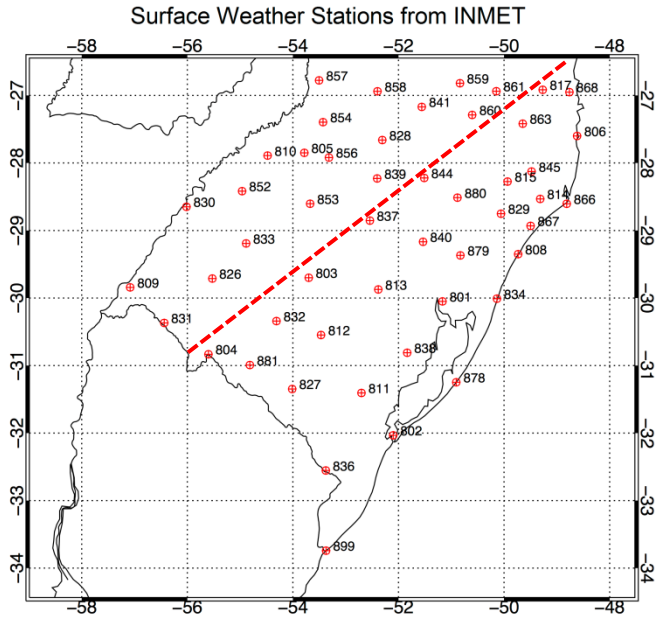

Fig. 12. Location of 50 surface weather stations from INMET. Each station has a WMO (World Meteorological Organization) code for identification purposes. The dashed red line separates the stations in two distinct groups for the analysis in section IV-B.

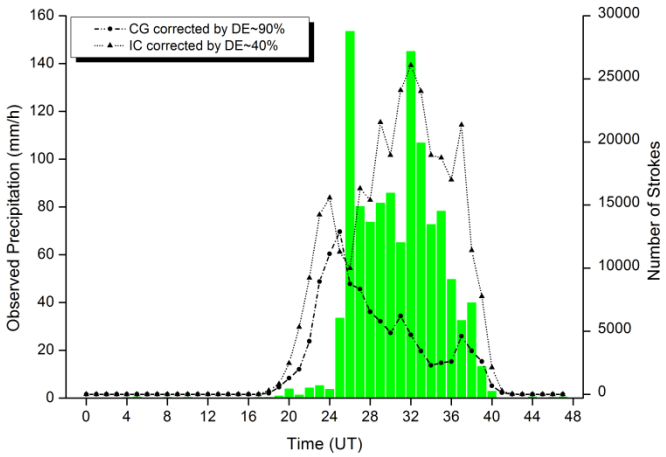

Fig. 13. Distribution of hourly-observed rainfall and CG and IC strokes.

IV. WEATHER RESEARCH AND FORECASTING (WRF) MODEL

The fully compressible and non-hydrostatic atmospheric WRF model version 3.3.1, coded with a terrain-following hydrostatic-pressure vertical coordinates [Skamarock et al., 2008], was implemented to process the simulations. As illustrated in Fig. 14, the model setup included a coarse 30 km grid (d01) (38.1327° to 21.9778° S and 64.205° to 42.308° W) and a nested 10 km grid resolution (d02) (34.4357° to 26.4458° S and 58.992° to 47.522° W). In the vertical direction, 27 unevenly spaced full sigma levels were established. The 0000

UT Global Forecast System (GFS) gridded analysis fields and 3-hour interval forecasts with 0.5° latitude×0.5° longitude horizontal grid resolution were used to initialize the model and nudge the boundaries of d01 during the 48-hour simulation period.

Four different convective parameterizations (CPs): the Kain–Fritsch scheme (KF) [Kain and Fritsch, 1990, 1993; Kain, 2004], the Betts–Miller–Janjic scheme (BM) [Janjic, 1994, 2000], the Grell–Devenyi ensemble scheme (GD) [Grell and Devenyi, 2002], and the New Grell 3D scheme (G3), which is an improved version of the GD scheme, were tested. In addition, we used Thompson graupel scheme [Thompson et al., 2008] for microphysics, and Rapid Radiative Transfer Model (RRTM) Longwave radiation [Mlawer et al., 1997] with the MM5 (Dudhia) Shortwave radiation scheme [Dudhia, 1989]. The Similarity Theory scheme [Dyer and Hicks, 1970; Paulson, 1970; Webb, 1970] was used to simulate surface layer fluxes, whereas the Yonsei University (YSU) PBL scheme [Hong et al., 2006] was used to simulate boundary layer fluxes. The land surface fluxes were obtained with the Noah LSM [Chen and Dudhia, 2001]. Different WRF simulations were performed in order to identify the cumulus scheme that represents more properly the intensity of the MCS precipitation. The WRF precipitation is a new variable that was incorporated into the Potential Lightning Region (PLR) tool.

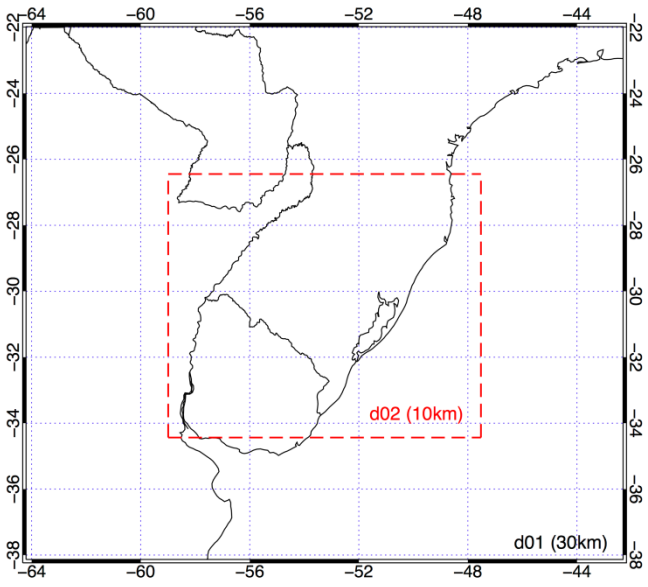

Fig. 14. The WRF domains: coarse domain (d01 – 30km) and nested domain (d02 – 10km). d02 is coincident with the study area showed in Fig. 1.

A. WRF Cumulus Schemes Vs. Precipitation

Only WRF grid points nearby the coordinates of the weather stations were chosen for this evaluation. The nearest-neighbor interpolation technique allowed the observed and simulated precipitation to be compared. Fig.15 is a composition of four multi-plot panels, one for each WRF CP tested. The graphs consist of a histogram, indicating the hourly model precipitation from WRF d02, a solid red curve, referring to hourly-observed precipitation from INMET stations, and a gray shaded area, showing the hourly average most unstable Convective Available Potential Energy (mCAPE).

Regardless of the CP used in the simulations, WRF produced false precipitation rates on the initial and final stages of the MCS. No CP has succeeded in reproducing the intensity of the two peaks observed precipitation in their proper time intervals. In general, the maximum mCAPE occurs before the time of the most intense rainfall, and as the CP converts the instability in convection the mCAPE decreases. Precipitation of KF is substantially delayed in time, and only one peak intensity was simulated. When a maximum of 153.4 mm was observed, model-precipitation was much underestimated. Considering the time after the second peak of the red curve, KF is the scheme that most overestimated rain intensity. BM was the only WRF parameterization that significantly underestimated the precipitation during the mature-to-dissipating stages of MCS. The two peaks in the observed data, although slightly underestimated in intensity and delayed in time, were well reproduced by WRF model using the GD scheme. Even the smaller peak between the maximum points of the red curve (at 30UT) can be identified in the purple histogram two hours later. The behavior of G3 scheme is similar to GD, including the temporal shift of the maximum values of precipitation. However, WRF with G3 shows small, almost constant variations in the precipitation intensity after the well-simulated first peak. Both parameterizations GD and G3 performed better in predicting the MCS precipitation.

Fig.16 consists of four graphics showing the hourly bias plots between observed and simulated precipitation, using different CPs. The observed precipitation was normalized by the mean value (26.4 mm/h) to be able to fit within the plot scale. According to the analysis of Fig.15, it was expected that the precipitation should be overestimated before and after the red curve for all CPs tested. During the raining stage of MCS, only BM significantly underestimated the precipitation intensity, and GD was the unique scheme to have more positive than negative bias. Regarding the highest amounts of observed precipitation, all CPs underestimated them.

The GD and G3 schemes simulated better the precipitation intensity and its temporal distribution when the MCS was more active. For the next analysis evolving the application of the PLR tool, GD is the designated parameterization for the WRF simulations.

B. Potential Lightning Region (PLR)

The lightning forecasting method called PLR (Lightning Potential Region) is a spatial distribution of lightning occurrence probabilities in a given area [Zepka et al., 2014]. It was defined based on a combination of WRF variables related mainly with the thunderstorm thermodynamics and obtained from WRF model. For the first time, PLR was tested in a region different from southeastern Brazil, where it was conceived and is used operationally. Lightning in southeastern Brazil is usually associated to local convective thunderstorms or frontal systems. Severe convective clusters, like MCSs occurring in the southern Brazil, have different dynamical mechanisms responsible for its formation and development, which are still not well known. To fit the PLR method for the meteorological scenario of the MCS, the tool proposed in Zepka et al. [2014] passed through some modifications.

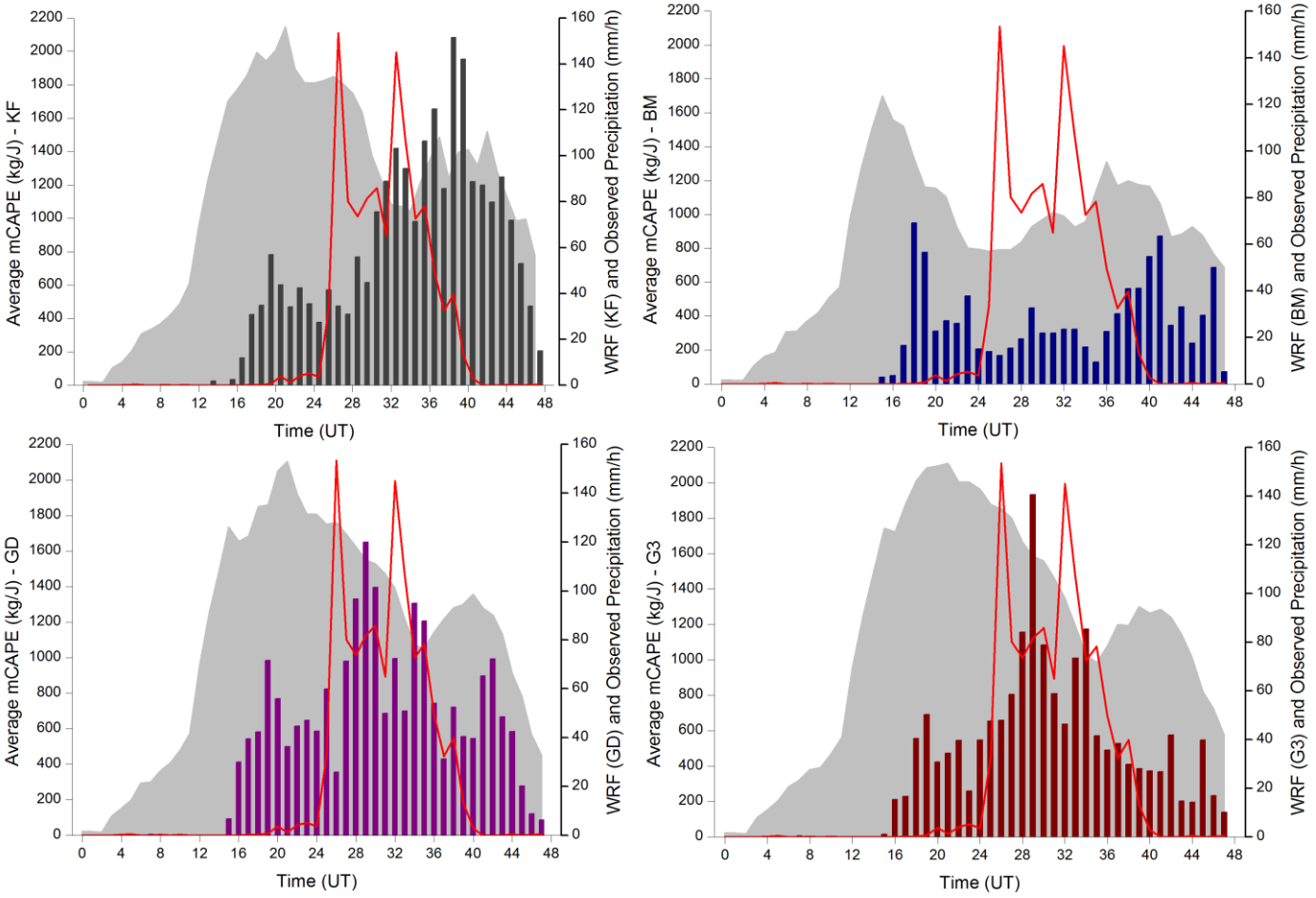

Fig. 15. Each multi-plot panel corresponds to WRF results obtained with a different convective parameterization (KF – Kain-Fritsch scheme, BM – Betts-Miller-Janjic scheme, GD – Grell-Devenyi ensemble scheme, G3 – New Grell 3D scheme). Histogram indicates the hourly model precipitation from WRF d02, solid red curve refers to hourly-observed precipitation from INMET stations, and gray shaded area shows the hourly average most unstable Convective Available Potential Energy (mCAPE).

First of all, new WRF variables were added to PLR formulation and others replaced in order to better represent the atmospheric dynamics. The following WRF model parameters were chosen to participate of PLR calculation: most unstable Convective Available Potential Energy, K-Index, Total Totals Index, 700-500 hPa lapse rate of equivalent potential temperature, 850-700 hPa vertical velocity average, vertical velocity at 500 hPa, relative vorticity at 500 hPa, omega at 500 hPa, divergence at 300 hPa, total precipitation, and 700-500 hPa ice-mixing ratio integrated.

The first version of PLR exhibited the forecasting results in terms of indices varying from 1 to 5. Those indices also represented increasing probabilities of lightning occurrence from <10% (index 1) to >90% (index 5). The new tool adds a non-lightning probability (0%). The renewed index range varies from 0 to 5, and values below an index of 1 are equivalent to non-lightning regions. Index increments of 0.5 correspond to 10% in lightning probabilities, starting from index 1 with a probability of 10%. Index 5 still corresponds to lightning probabilities greater than 90%; there is not yet a 100% lightning probability assigned by PLR. Also in the first PLR, WRF variable value ranges were transformed into discrete indices (1, 2, 3, 4 or 5) for calculation purposes (see Zepka et al. [2014] for more details). Now, float point values (from 0.01 to 4.99) are attributed to the variables, improving the quality of the final results. Any suggestions for changes that were briefly commented, and then implemented to generate the PLR maps over southern Brazil for the MCS, are still developing. A detailed report of all improvements in PLR method will be available shortly in a Journal version.

Fig. 17 exemplifies PLR maps in different circumstances during the overall period analyzed. The black dots are the location of CG and IC (total lightning) strokes. Fig. 17(a) represents a situation of non-lightning region, but is possible to observe a small (<30%) chance of lightning occurrence over northern RS state and southern Paraguay. This can be explained with the help of Figs. 18 and 19. They show significant thermodynamic features of the lower atmosphere, which probably should have induced higher values of PLR. The fields of composite-variables in the figures were simulated in WRF model for 30 km (d01) grid resolution. Observing the inclination of 1000-500 hPa layer thickness lines in Fig.18, it is possible to note a differential warming of the lower-middle troposphere. Over the continent, warm air extended from

Argentina to southeastern Brazil, and its core was coupled to the Northwestern Argentinean Low (NAL) [Seluchi and Saulo, 2012] located at 33°S/65°W (not shown). In Fig. 19, it is observed a southward flow of moisture in lower levels transported by SALLJ. Despite a mass of dry air has predominated in almost all RS state, the extreme north region was under the influence of a trough associated with the NAL, showing high values of relative humidity. The same was verified over the southern Paraguay, where the small PLR probabilities were also found.

In Fig. 17(b), PLR succeeded in reproducing the position of total lightning activity over southwestern RS. Except for the region marked in red over northeastern Argentina, where no lightning was observed, PLR appropriately inferred low probabilities to the remaining domain. Few strokes happened in the white area over Atlantic Ocean, but, in general, the non-lightning region was conserved.

On PLR map of Fig. 17(c), there is a spatial displacement between the total lightning activity and the regions assigned with high probabilities of lightning occurrence. PLR map seems to show a delay in MCS propagation in the southeastern portion of the domain. A probable reason for this spatial error might be related to the winds profile. If this is true, WRF model is, in fact, responsible for the propagation delay. In order to test this hypothesis, surface wind direction data from the INMET stations were investigated. According to Fig. 12, the dashed red line divided the weather stations into two distinct groups. The northwestern region from RS state had 19 stations and was called as group#1. The southeastern region received the name of group#2 and is comprised by 31 stations. Fig. 20 presents the wind roses built with observed and WRF simulated wind direction data only for the period in which the spatial error was detected (from 04UT to 18UT of December 11th 2012). In the case of Fig. 20(a) (group#1), the agreement between the two wind roses is good and the northwest wind direction dominates. In Fig. 20(b) (group#2), both wind roses showed leading northwest wind direction, but WRF model underestimated the southwest direction and overestimated the north one. The MCS came from southwest, so if the WRF did not simulate properly the wind direction responsible by MCS propagation, it would expect that a spatial mismatch would occur between PLR maps and total lightning locations.

Finally, PLR map in Fig. 17(d) showed a large white area that increased as the probabilities of lightning occurrence were reduced after the passage of MCS. Very few discharges were identified in this region. In spite of total lightning strokes were spread even over regions with PLR values smaller than 30%, areas with higher probabilities were also associated.

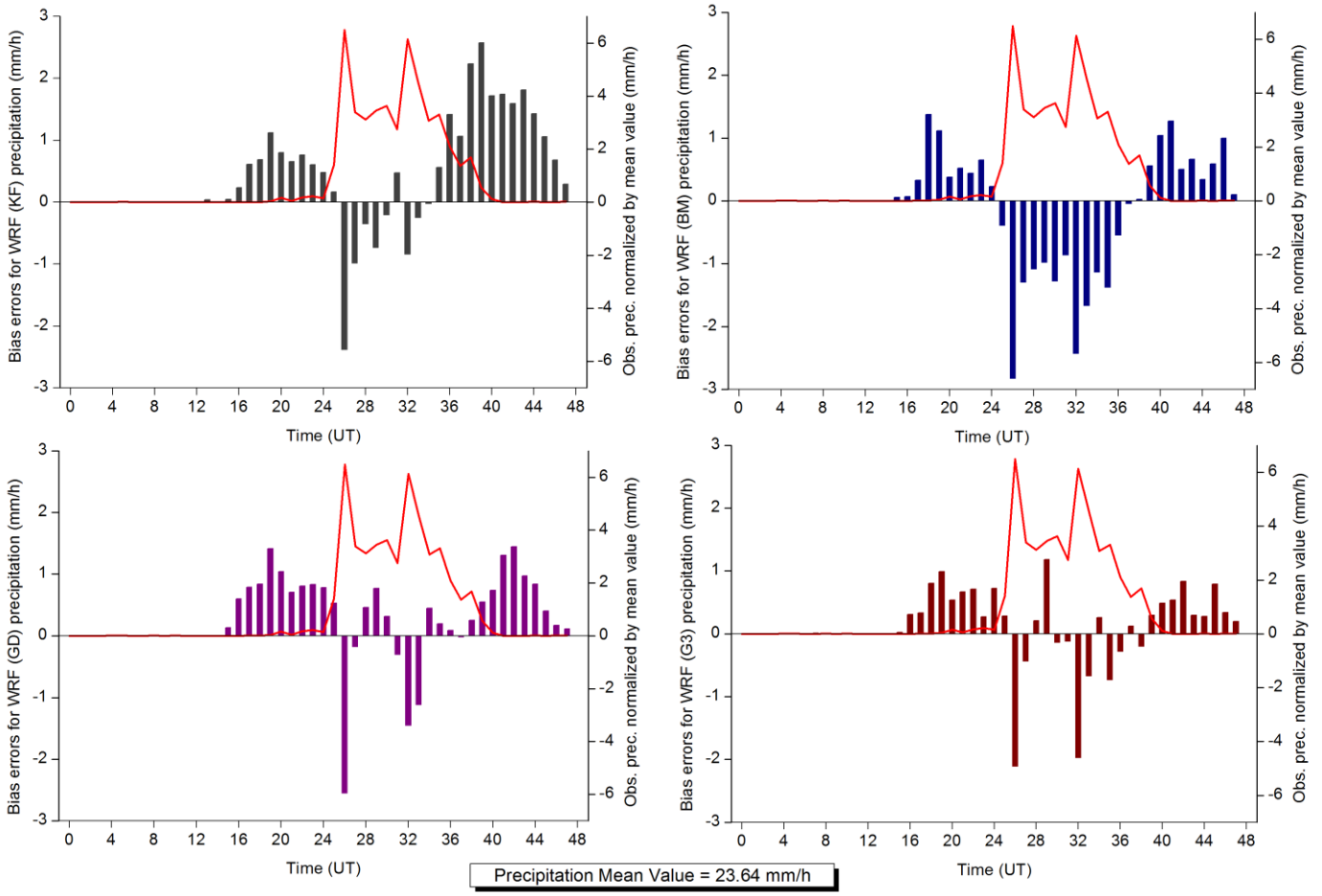

Fig. 16. Bias histograms for WRF precipitation simulated with different convective parameterizations (KF – Kain-Fritsch scheme, BM – Betts-Miller-Janjic scheme, GD – Grell-Devenyi ensemble scheme, G3 – New Grell 3D scheme). Solid red curve represents the hourly-observed precipitation from INMET stations normalized by the mean value (23.64 mm/h).

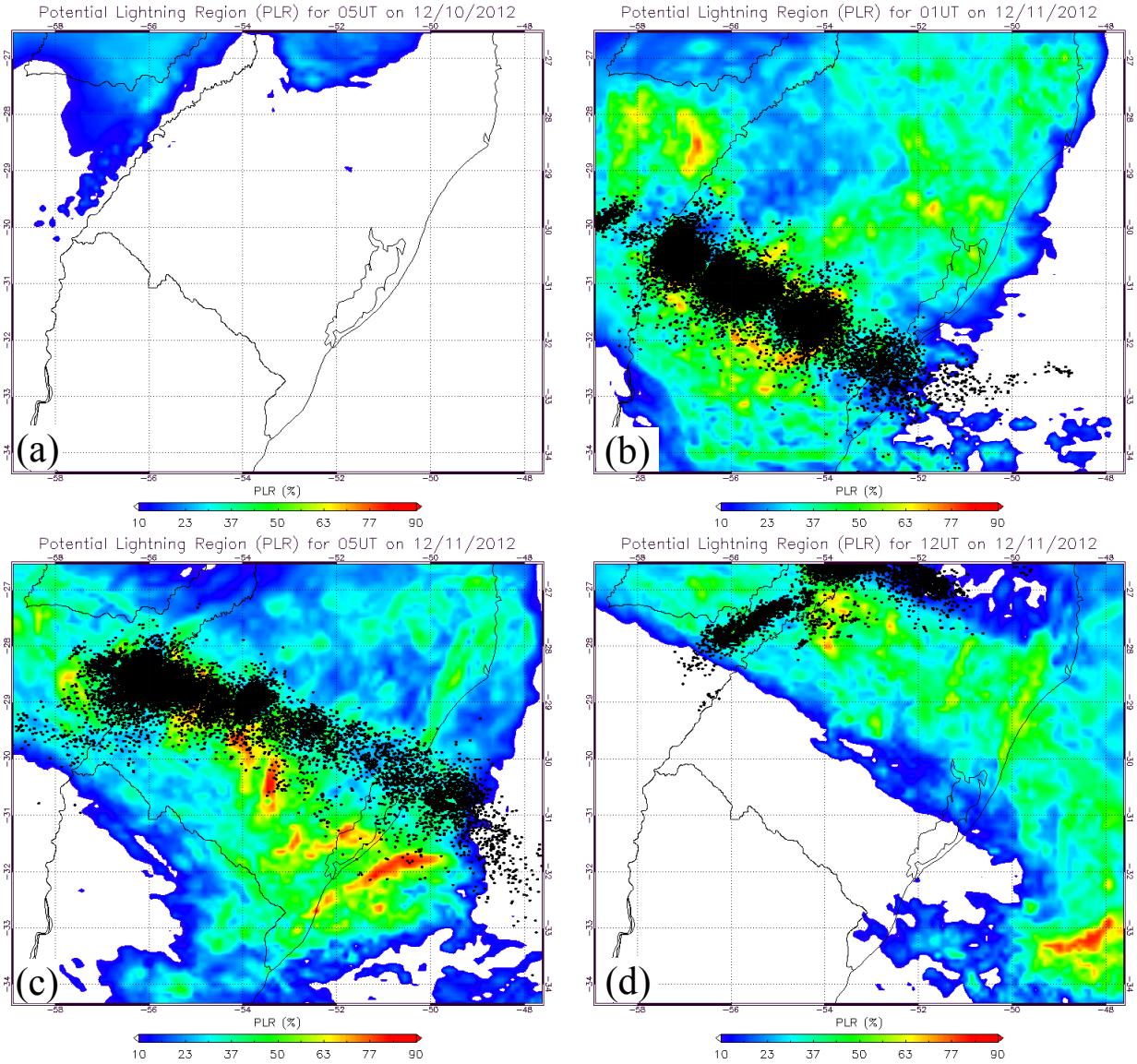

Fig. 17. Examples of PLR maps in different times during the overall period analyzed: (a) non-lightning region; (b) high PLR probabilities associated with total lightning activity; (c) spatial mismatch between lightning and high PLR; (d) end of total lightning activity and non-lightning region forthcoming. The black dots represent the location of CG and IC (total lightning) strokes.

V. SUMMARY AND CONCLUSIONS

In this work, the performance of WRF model in predicting heavy rainfall and strong lightning activity associated to convective storms of a huge mesoscale convective system (MCS) that occurred over southern Brazil in the middle of December 2012 was investigated. For this purpose, 48-hours simulations were performed using four different WRF convective parameterizations. Forecasting extreme precipitation events is usually a difficult task from both spatial and temporal sights. For the MCS analyzed, WRF showed phase errors and the precipitation was depicted off in time by a few hours. Using observed data from 50 weather stations homogenously distributed over the WRF domain, temporal bias errors were calculated. WRF underestimated maximum values of precipitation even considering the distribution shifted in time. The Grell-Devenyi (GD) parameterization was chosen for the study of lightning forecasting.

Between CG and IC discharges, BrasilDAT detected more than 220,000 strokes while the MCS passed through Rio Grande do Sul (RS) state. As the detection efficiency (DE) of BrasilDAT is different for CG and IC, both rates were corrected, and the total amount of discharges has increased considerably, especially of IC. The maximum value of IC/CG ratio was 8.2. 4% of the 97,696 CG strokes presented absolute values of peak current greater than 75 kA, leading those of negative polarity. Potential Lightning Region (PLR) is a lightning forecasting method developed using exclusively the WRF model. For the first time, the tool was applied to a region different of southeastern Brazil, where it was conceived and is used operationally.

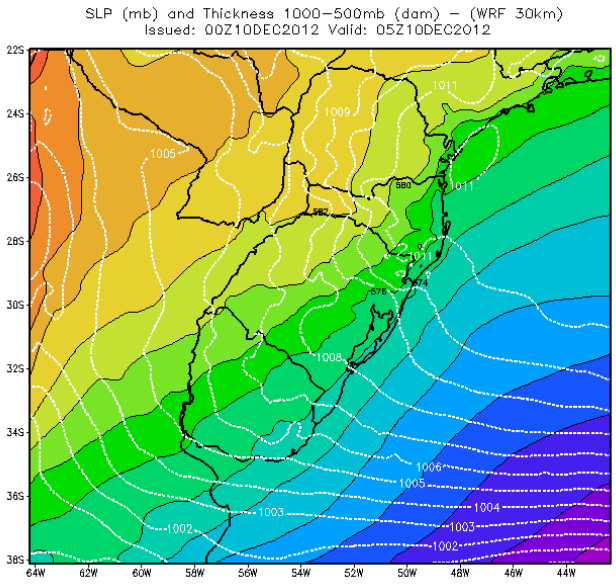

Fig. 18. Sea Level Pressure (SLP) and 1000-500 hPa thickness simulated in WRF model (30 km) for the same time of Fig.17(a).

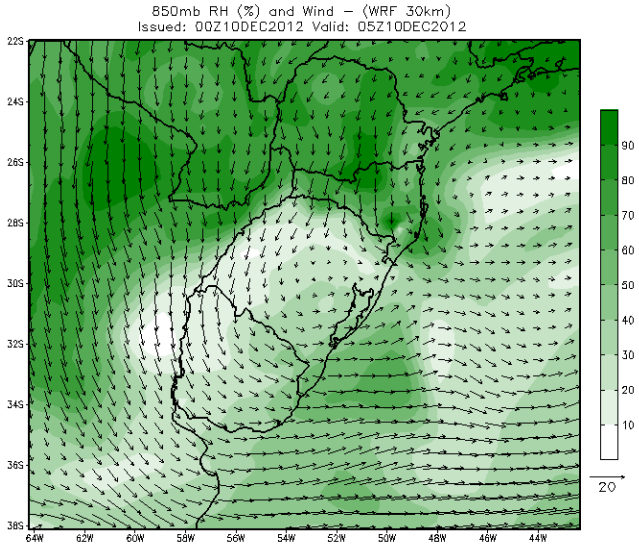

Fig. 19. Relative Humidity (RH) and wind vectors at 850 hPa simulated in WRF model (30 km) for the same time of Fig.17(a).

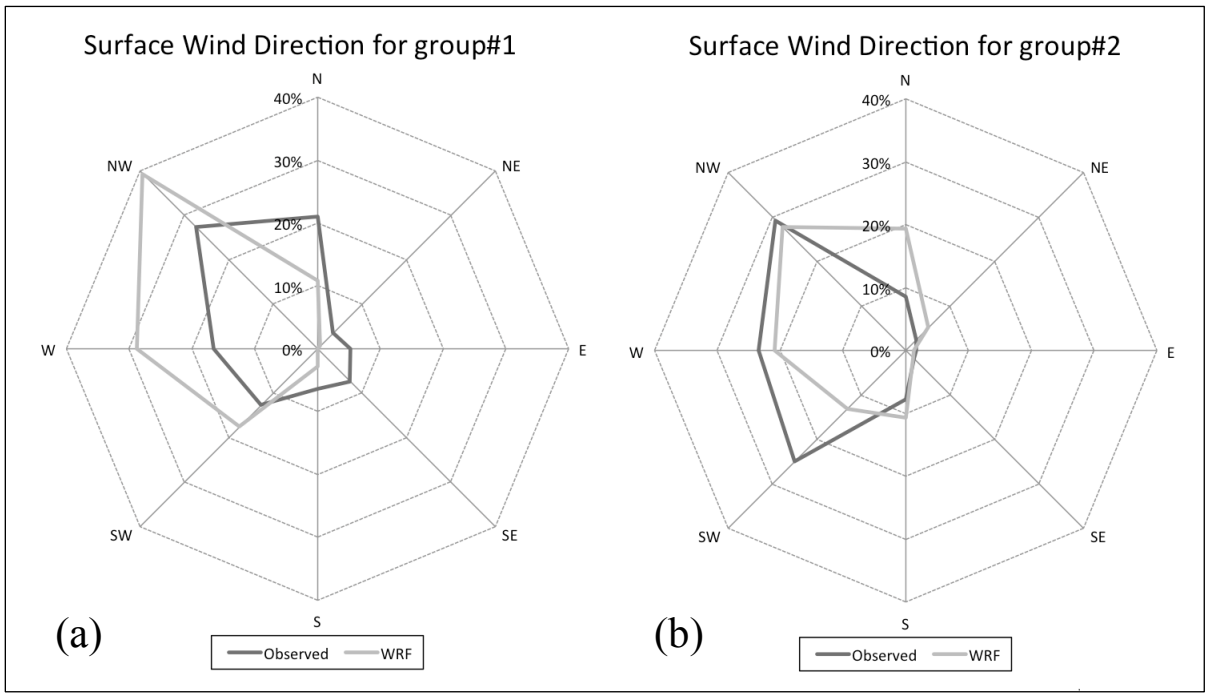

Fig. 20. Wind roses built with observed and WRF simulated wind direction data: (a) for the northwestern region from RS state (19 weather stations, group #1); (b) for the southeastern region (31 weather stations, group#2).

For this work, PLR tool has undergone certain modifications regarding the WRF variables in order to assign a more significant dynamic component into its formulation previously dominated by the thermodynamics. A relevant characteristic of the new PLR was the addition of a non-lightning probability, which represents a commitment in highlighting regions with 0% chance of lightning occurrence. All improvements in PLR method that were commented in the text and implemented for this study case are a work in progress. Shortly a PLR refresh version will be submitted for publication. Four PLR maps were shown to illustrate different statuses of the lightning forecasting: (a) a non-lightning region; (b) high PLR probabilities associated with total lightning activity; (c) spatial mismatch between lightning and high PLR; (d) end of total lightning activity and non-lightning region forthcoming. For the dissimilarities verified in (a) and (c) between PLR maps and the total lightning occurrence, possible reasons were suggested. In general, despite the WRF limitation in reproducing properly the surface wind direction, PLR was an efficient tool for forecasting lightning in southern Brazil.

REFERENCES

Abdoulaev, S., Marques, V. S., Pinheiro, F., Martinez, E. F., Lenskaia, O. (2001), Analysis of mesoscale system using cloud-to-ground flash data, Revista Brasileira de Geofisica, 19(1), 75-95.

Carey, L. D., Murphy, M. J., McCormick, T. L., Demetriades, N. W. (2005), Lightning location relative to storm structure in a leading-line, trailing-stratiform mesoscale convective system, J. Geophys. Res., 110(D3).

Chen, F., Dudhia, J. (2001), Coupling an advanced land surface-hydrology model with the Penn State-NCAR MM5 modeling system. Part I: Model implementation and sensitivity, Mon. Wea. Rev., 129(4), 569-585.

Corfidi, S. F., Meritt, J. H., Fritsch, J. M. (1996), Predicting the movement of mesoscale convective complexes. Wea. Forecast., 11(1), 41-46.

Dudhia, J. (1989), Numerical study of convection observed during the winter monsoon experiment using a mesoscale two-dimensional model, J. Atmos. Sci., 46(20), 3077-3107.

Dyer, A. J., Hicks, B. B. (1970), Flux-gradient relationships in the constant flux layer, Quart. J. Roy. Meteor. Soc., 96(410), 715-721.

Goodman, S. J., MacGorman, D. R. (1986), Cloud-to-ground lightning activity in mesoscale convective complexes, Mon. Wea. Rev., 114(12), 2320-2328.

Grell, G. A., Devenyi, D. (2002), A generalized approach to parameterizing convection combining ensemble and data assimilation techniques, Geophys. Res. Lett., 29 (14), 1693.

Holle, R. L., Watson, A. I., López, R. E., Macgorman, D. R., Ortiz, R., Otto, W. D. (1994), The life cycle of lightning and severe weather in a 3-4 June 1985 PRE-STORM mesoscale convective system. Mon. Wea. Rev., 122(8), 1798-1808.

Hong, S. Y., Lim, J. O. J. (2006), The WRF single-moment 6-class microphysics scheme (WSM6), J. Korean Meteor. Soc, 42(2), 129-151.

Houze, R. A. (1993), Cloud Dynamics. Academic Press, 573pp.

Janjic, Z. I. (1994), The step-mountain eta coordinate model: further development of the convection, viscous sublayer, and turbulent closure schemes, Mon. Weather Rev., 122, 927-945.

Janjic, Z. I. (2000), Comments on "Development and evaluation of a convection scheme for use in climate models", J. Atmos. Sci., 57, 3686.

Kain, J. S. (2004), The Kain–Fritsch convective parameterization: an update, J. Appl. Meteorol., 43, 170-181.

Kain, J. S., Fritsch, J. M. (1990), A one-dimensional entraining/detraining plume model and its application in convective parameterization, J. Atmos. Sci., 47, 2784-2802.

Kain, J. S., Fritsch, J. M. (1993), Convective parameterization for mesoscale models: the Kain–Fritsch scheme, The Representation of Cumulus in Numerical Models, 46, Amer. Meteor. Soc, Boston, pp. 165-177.

Keighton, S. J., Bluestein, H. B., MacGorman, D. R. (1991), The evolution of a severe mesoscale convective system: Cloud-to-ground lightning location and storm structure, Mon. Wea. Rev., 119(7), 1533-1556.

Lyons, W. A., Uliasz, M., Nelson, T. E. (1998), Large peak current cloud-to-ground lightning flashes during the summer months in the contiguous United States, Mon. Wea. Rev., 126(8).

MacGorman, D. R., Morgenstern, C. D. (1998), Some characteristics of cloud-to-ground lightning in mesoscale convective systems, J. Geophys. Res., 103(D12), 14011-14023.

Machado, L. A. T., Rossow, W. B., Guedes, R. L., Walker, A. W. (1998), Life cycle variations of mesoscale convective systems over the Americas, Mon. Wea. Rev., 126(6).

Marengo, J. A., Soares, W. R., Saulo, C., Nicolini, M. (2004), Climatology of the Low-Level Jet East of the Andes as Derived from the NCEP–NCAR Reanalyses: Characteristics and Temporal Variability, J. Climate, 17(12).

Mattos, E. V., Machado, L. A. (2011), Cloud-to-ground lightning and Mesoscale Convective Systems, Atmos. Res., 99(3), 377-390.

Mlawer, E. J., Taubman, S. J., Brown, P. D., Iacono, M. J., Clough, S. A. (1997), Radiative transfer for inhomogeneous atmospheres: RRTM, a validated correlated-k model for the longwave, J. Geophys. Res., 102(D14), 16663-16682.

Naccarato, K. P., Saraiva, A. C. V., Saba, M. M. F., Schumann, C., Pinto Jr, O. (2012), First performance analysis of BrasilDAT total lightning network in southeastern Brazil, Proceedings of the International Conference on Grounding and Earthing (GROUND'2012) & 5th International Conference on Lightning Physics and Effects (LPE), CD-ROM, Bonito.

Nesbitt, S. W., Zipser, E. J., Cecil, D. J. (2000), A census of precipitation features in the Tropics using TRMM: Radar, ice scattering, and lightning observations, J. Climate, 13(23).

Orville, R. E., Henderson, R. W., Bosart, L. F. (1988), Bipole patterns revealed by lightning locations in mesoscale storm systems, Geophys. Res. Lett., 15(2), 129-132.

Parker, M. D., Rutledge, S. A., Johnson, R. H. (2001), Cloud-to-ground lightning in linear mesoscale convective systems, Mon. Wea. Rev., 129(5), 1232-1242.

Paulson, C. A. (1970), The mathematical representation of wind speed and temperature profiles in the unstable atmospheric surface layer, J. Applied Meteor., 9(6), 857-861.

Pinto Jr, O., Pinto, I. R. C. A., Naccarato, K. P. (2007), Maximum cloud-to-ground lightning flash densities observed by lightning location systems in the tropical region: A review, Atmos. Res., 84(3), 189-200.

Pinto Jr., O., Saba, M. M. F., Pinto, I. R. C. A., Tavares, F. S. S., Naccarato, K. P., Solorzano, N. N., Taylor, M. J., Pautet, P. D., Holzworth, R. H. (2004), Thunderstorm and lightning characteristics associated with sprites in Brazil, Geophys. Res. Lett., 31(13).

Rutledge, S. A., MacGorman, D. R. (1988), Cloud-to-ground lightning activity in the 10-11 June 1985 mesoscale convective system observed during the Oklahoma-Kansas PRE-STORM project, Mon. Wea. Rev., 116(7), 1393-1408.

Seluchi, M. E., Saulo, A. C. (2012), Baixa do Noroeste Argentino e Baixa do Chaco: Caracterísiticas, Diferenças e Semelhanças, Revista Brasileira de Meteorologia, 27(1), 49-60.

Silva, V., Berbery, E. H. (2006), Intense rainfall events affecting the La Plata Basin, J. Hydrometeor., 7(4).

Siqueira, J. R., Rossow, W. B., Machado, L. A. T., Pearl, C. (2005), Structural Characteristics of Convective Systems over South America Related to Cold-Frontal Incursions, Mon. Wea. Rev., 133(5).

Skamarock, W. C., Klemp, J. B., Dudhia, J., Gill, D. O., Barker, D. M., Duda, M. G., Huang, X-Y., Wang, W., Powers, J. G. (2008), A description of the Advanced Research WRF Version 3, NCAR Tech. Notes.

Teixeira, M. D. S., Satyamurty, P. (2007), Dynamical and Synoptic Characteristics of Heavy Rainfall Episodes in Southern Brazil, Mon. Wea. Rev., 135(2).

Thompson, G., Field, P. R., Rasmussen, R. M., Hall, W. D. (2008), Explicit forecasts of winter precipitation using an improved bulk microphysics scheme. Part II: Implementation of a new snow parameterization, Mon. Wea. Rev., 136(12).

Velasco, I., & Fritsch, J. M. (1987), Mesoscale convective complexes in the Americas, J. Geophys. Res., 92(D8), 9591-9613.

Vera, C., Baez, J., Douglas, M., Emmanuel, C. B., Marengo, J., Meitin, J., Nicolini, M., Noegues-Paegle, J., Paegle, J., Penalba, O., Salio, P., Saulo, C., Silva Dias, M. A. F., Silva Dias, P., Zipser, E. (2006), The South American low-level jet experiment, Bull. Amer. Meteor. Soc., 87(1).

Webb, E. (1970), Profile relationships: The log-linear range, and extension to strong stability, Quart. J. Roy. Meteor. Soc., 96(407), 67-90.

Zepka, G. S., Pinto Jr, O., Saraiva, A. C. V. (2014), Lightning forecasting in southeastern Brazil using the WRF model, Atmos. Res., 135, 344-362.

Zipser, E. J., Cecil, D. J., Liu, C., Nesbitt, S. W., Yorty, D. P. (2006), Where are the most intense thunderstorms on Earth?, Bull. Amer. Meteor. Soc., 87(8).